

10. SEISMIC STRATIGRAPHY IN A TRANSVERSE RIDGE, ATLANTIS II FRACTURE ZONE¹

Stephen A. Swift,² Hartley Hoskins,² and Ralph A. Stephen²

ABSTRACT

During Ocean Drilling Program Leg 118, we conducted a vertical seismic profile in Hole 735B, a 0.5-km-deep borehole in 720 m of water on the eastern wall of the Atlantis II Fracture Zone, Southwest Indian Ridge. Seismograms were collected at 20 borehole depths, alternately using a water gun and then an air gun at each depth. The overall velocity is 6.5 km/s. The lowest interval velocities occur in the foliated gabbros (lithologic Unit I) and olivine gabbro-troctolite (Unit VI). We separated up- and down-going wavefields with frequency-wave number filtering and deconvolved the up-going field by spectral division using the down-going field at each receiver depth. The processed sections show irregular reflections from the base of the foliated gabbros (Unit I, 50–70 mbsf) and from the Fe-Ti rich gabbro (Unit IV, 225–250 mbsf). We tentatively interpret coherent events at ~560 and 760–825 mbsf as reflections from Moho raised tectonically to shallow depths within the transverse ridge.

INTRODUCTION

During Leg 118, scientists drilled a 0.5-km-deep hole at Site 735 on the crest of the eastern transverse ridge paralleling the Atlantis II Fracture Zone (Shipboard Scientific Party, 1989). Coring recovered a suite of layered olivine-gabbro rocks having lithologic and geochemical similarities to lower ocean-crust gabbros observed in ophiolites (e.g., Casey et al., 1981) and in fracture zones (e.g., Karson and Fox, 1986). Rock velocities averaging 6.5 to 6.8 km/s, measured by laboratory apparatus, sonic logging, and vertical seismic profiling (Shipboard Scientific Party, 1989) are similar to well-constrained refraction velocities from ocean layer 3 (e.g., Spudich and Orcutt, 1980) and confirm the lower crustal origin of the drilled section.

Vertical and lateral variations in seismic structure of lower oceanic crust have been observed by multichannel reflection and refraction techniques. Away from fracture zones, laminated zones and dipping reflectors spaced 5- to 10-km apart appear in lower crustal portions of multichannel profiles (NAT Group, 1985; McCarthy et al., 1988; White et al., 1988). On slow-spreading ridges, refraction data indicate that the variability of crustal and Moho seismic structure increases near fracture zones (Detrick and Purdy, 1980; Cormier et al., 1984; Mutter et al., 1984; White et al., 1984; Minshull et al., 1988). These data suggest that beneath fracture zone troughs the crust is often thinner, velocities are lower, and ocean layer 3 velocities (6.8 to 7.1 km/s) are uncommon. Alternatively, McCarthy et al. (1988) observed that Moho in a reflection profile deepened with proximity to the Blake Spur Fracture Zone, and Karson and Elthon (1987) used an analogy with the Bay of Islands ophiolite to propose that the depth to the base of the magmatic layer does not change with distance from fracture zones.

Few reflection or refraction studies of fracture zones have investigated the structure of transverse ridges, such as that drilled at Site 735. Detrick and Purdy (1980) used mantle delay times to infer that anomalously thin crust at the Kane Fracture Zone extended beneath the northern transverse ridge. McCarthy et al. (1988) observed a flat, mid-crustal reflector beneath the ridge separating the northern and southern Blake Spur

fracture zones, but saw no shallowing of the Moho reflector. Neither multichannel reflection data nor refraction data were collected at Site 735.

We performed a vertical seismic profile (VSP) in Hole 735B to obtain interval velocities at seismic frequencies and length scales, to estimate physical properties, and to record reflections. VSP traveltimes were reported by the Shipboard Scientific Party of Leg 118 (1989). Here, we correlate smoothed interval velocities with borehole lithology, whereas Kirby et al. (unpubl. data) compared smoothed VSP velocities with velocities from laboratory and sonic logging. We also discuss signal processing techniques used on the data and report results of separating the reflected wavefield from the stacked VSP seismograms.

METHODS

The Shipboard Scientific Party of Leg 118 (1989) described the methods used to collect VSP data at Site 735. We acquired the VSP by clamping a three-component seismometer at 23 borehole depths and by shooting alternately with a 1000-in.³ air gun and a 400-in.³ water gun suspended from a floating buoy at 8.7 and 4.8 mbsl, respectively. Although the end of the drill pipe was not clamped to the reentry cone as during ODP Legs 104 and 111 as a result of operational constraints, inspection of seismograms for transient events indicated that pipe banging was an important source of noise only when the seismometer was clamped in the upper 50 to 80 m of the borehole. The signals from a source monitor hydrophone deployed at 250 mbsl and the three seismometer channels were recorded in the Underway Geophysics Laboratory on board the *Resolution* at a digitization rate of 1000 Hz for 4 s after anti-alias filtering at 250 Hz. We discarded data at the three deepest tool locations because tool slippage severely degraded the signal-to-noise ratio. We processed data from 20 clamping depths. The depth interval between tool locations was most often 25 ± 2 m (12 intervals), but ranged from 15 (3 intervals) to 31 m (1 interval) and averaged 23 m. Hardage (1983) discussed depth-spacing requirements to avoid spatial aliasing. At a spacing of 23 m, frequencies greater than 98 Hz are spatially aliased for seismic velocities greater than 4.5 km/s (the minimum sonic velocity, Unit IV). Figure 1 shows spectra from both sources at the source monitor and at the uppermost receiver.

We also used the Schlumberger WST (vertical component only) seismometer to record a separate VSP (Shipboard Scien-

¹ Von Herzen, R. P., Robinson, P. T., et al., 1991. *Proc. ODP, Sci. Results*, 118: College Station, TX (Ocean Drilling Program).

² Woods Hole Oceanographic Institution, Woods Hole, MA 02543, U.S.A.

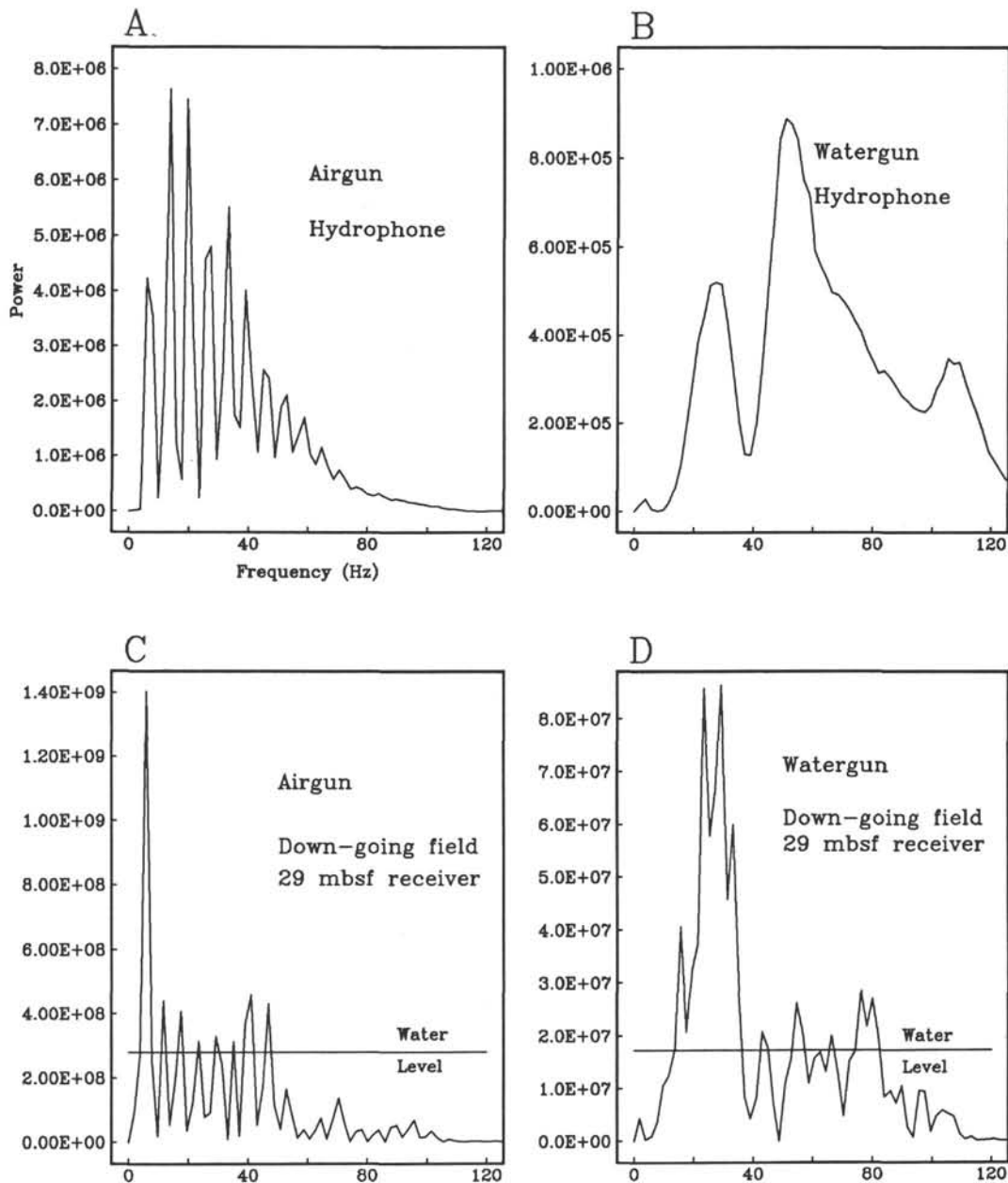


Figure 1. Air- and water-gun source power spectra. Magnitude of vertical scale has only relative significance. A., B. Spectra of 0.5-s records from source monitor at 250 mbsl. C., D. Spectra of 0.5-s portion of down-going wavefield recorded at uppermost receiver and separated by F-K filtering. "Water level" is the minimum amplitude (0.2 times the maximum amplitude) allowed in each frequency bin during spectral division deconvolution.

tific Party, 1989). The clamping depths were erratically spaced. Therefore, these data are unsuitable for frequency-wave number (F-K) velocity filtering and are not discussed in this paper.

Logging the hole with an inclinometer showed maximum hole deviation of 6° from vertical at azimuths between 0° and 40° (Fig. 72 in Shipboard Scientific Party, 1989). During the VSP, the ship's heading was maintained between 30° and 40° , and the moon pool was held within a few meters offset from the guidebase. Using these data and the deck geometry of the experiment from Figure 94 in Shipboard Scientific Party (1989), the horizontal separation between gun and receiver varied from only ~ 50 m at shallow clamping depths to ~ 100 m at the bottom of the hole.

A number of problems occurred while collecting the VSP that adversely affected data quality. It was often difficult to obtain secure attachment of the seismometer to the wall of the borehole. Inspection of borehole televiewer records showed that the interior surface of the borehole was relatively crack-free. The points on the tool clamping arm probably slipped on the polished wall. Slipping of the tool degraded the data quality at depths below 400 mbsf. The data from the three deepest stations (greater than 480 m) were not processed for this reason, and the data from stations at 415, 434, and 465 mbsf were only marginally acceptable. The direct wave triggered ringing on both horizontal geophones. At most depths, this ringing dominated the 2- to 80-Hz band of seismic

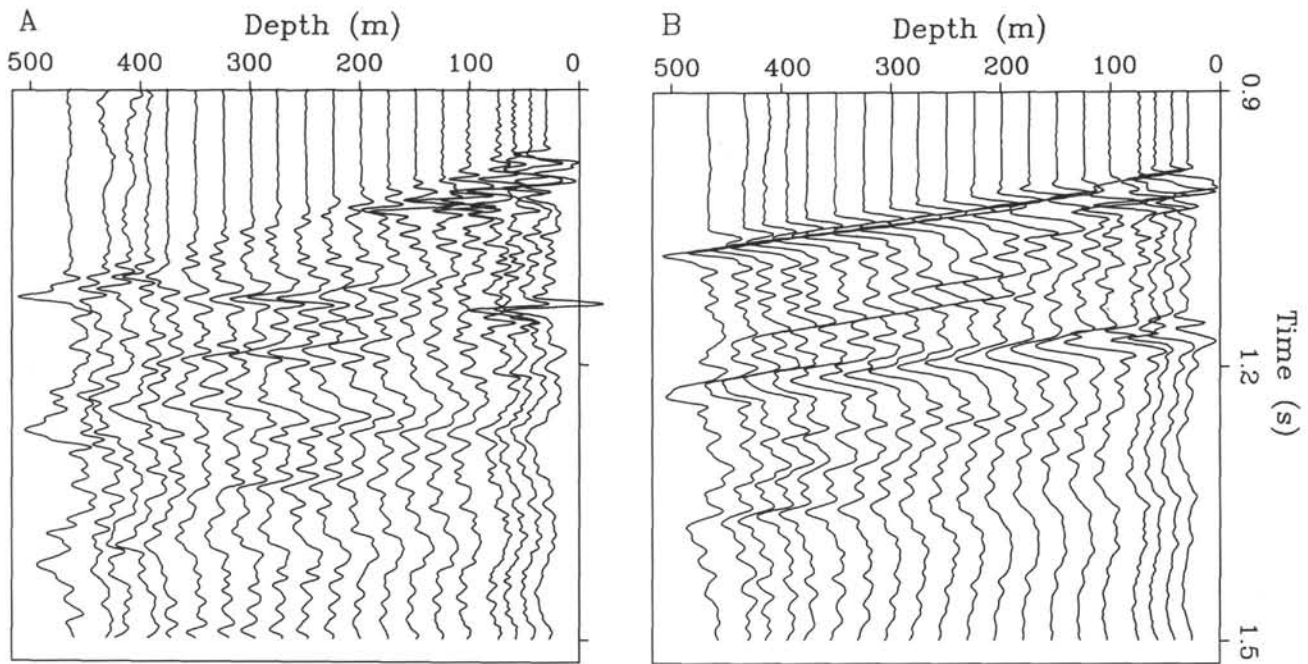


Figure 2. Airgun record sections processed by stacking and F-K filtering. Horizontal scale is depth of receiver below seafloor. **A.** Up-going wavefield. Timing for each seismogram has been increased by the one-way traveltime to each receiver depth. Reflections from flat, laterally continuous impedance contrasts should have the same arrival time at each receiver depth. **B.** Down-going wavefield. Timing has not been adjusted.

interest. For this reason, data from the horizontal geophones were not processed beyond the stacking and filtering reported by the Shipboard Scientific Party (1989). During data recording, the analog-digital converter clipped high amplitude peaks in the air-gun signal recorded on the vertical channel at the six shallowest clamping stations above 125 mbsf. Because the water gun produced less power, the signals recorded at these depths from the water gun were not clipped. Last, the blast phone timing functions did not work for most of the experiment. Recording was triggered by the firing pulse to the active gun. We made static corrections to adjust the timing to the first pulse, but did not correct for the 32- to 36-ms separation between the main pulses of the water and air guns (Shipboard Scientific Party, 1989). Figure 93 in Shipboard Scientific Party (1989) shows an apparent offset in first arrival caused by the delay in the main pulse of the water gun.

DATA PROCESSING

The data presented here were processed in four steps: (1) trace editing and vertical stack, (2) static timing corrections, (3) spherical spreading amplitude correction and separation of up- and down-going energy, and (4) spiking deconvolution of the up-going trace. The first two steps were discussed in Shipboard Scientific Party (1989) and Lee and Balch (1983).

We separated up- and down-going energy with a frequency-wave number (F-K) filter (Hardage, 1983; Christie et al., 1983). This method assumes constant spacing of seismometer stations. We chose this method, despite the variation in spacing of 15 to 30 m during our experiment, because of the ease with which the method could be implemented and used. Using this method with uneven receiver spacing may distort waveforms. We did not interpolate our data to constant depth spacing because this approach also can distort waveforms. As part of any future work on this data set, we will model our

depth sampling with synthetic seismograms to estimate the extent of distortion introduced by assuming constant receiver spacing. Before transforming our data, we removed frequencies above 100 Hz to avoid spatial aliasing and scaled the data with $D \cdot \exp(\alpha \cdot D)$, where α is an attenuation parameter and D is borehole depth, to compensate for geometrical spreading and attenuation effects (Lee and Balch, 1983). We chose a value of 0.6 for α to obtain approximately constant root-mean-square values in the upper 1.0 s. About 2 s of data at 20 depths was processed. We tapered the edges of the velocity template with cosine ramps 100 points long in frequency and six points long in wave number. Figures 2 and 3 show both wavefields for the air- and water-gun data, respectively.

We deconvolved the up-going trace by the spectral division method using the down-going trace at each depth as the inverse operator. Ross and Shah (1987) pointed out that the deconvolved trace is zero phase, that the method removes differences in coupling at different depths, and that each deconvolved trace is a representation of only the material properties and thicknesses below its clamping depth. This method corrects the difference in timing between the main pulse of the air and water guns. Our implementation used the "water level" method of Dey-Sarker and Wiggins (1976) and Langston (1979) to reduce noise introduced at frequencies where the amplitude of the down-going trace was low. By trial and error we found that setting the minimum amplitude of the spectrum in the denominator to 0.2 times the maximum amplitude achieved the best tradeoff between reducing noise and losing high-frequency resolution. Figures 1C and 1D show how this correction affects the spectra of the down-going trace. Likewise, we found that events on the deconvolved traces were best resolved when we used only the primary down-going pulse as the inverse operator, not the entire down-going trace. Inspection of the down-going seismograms (Figs. 2B and 3B) shows that for the water gun, a window of

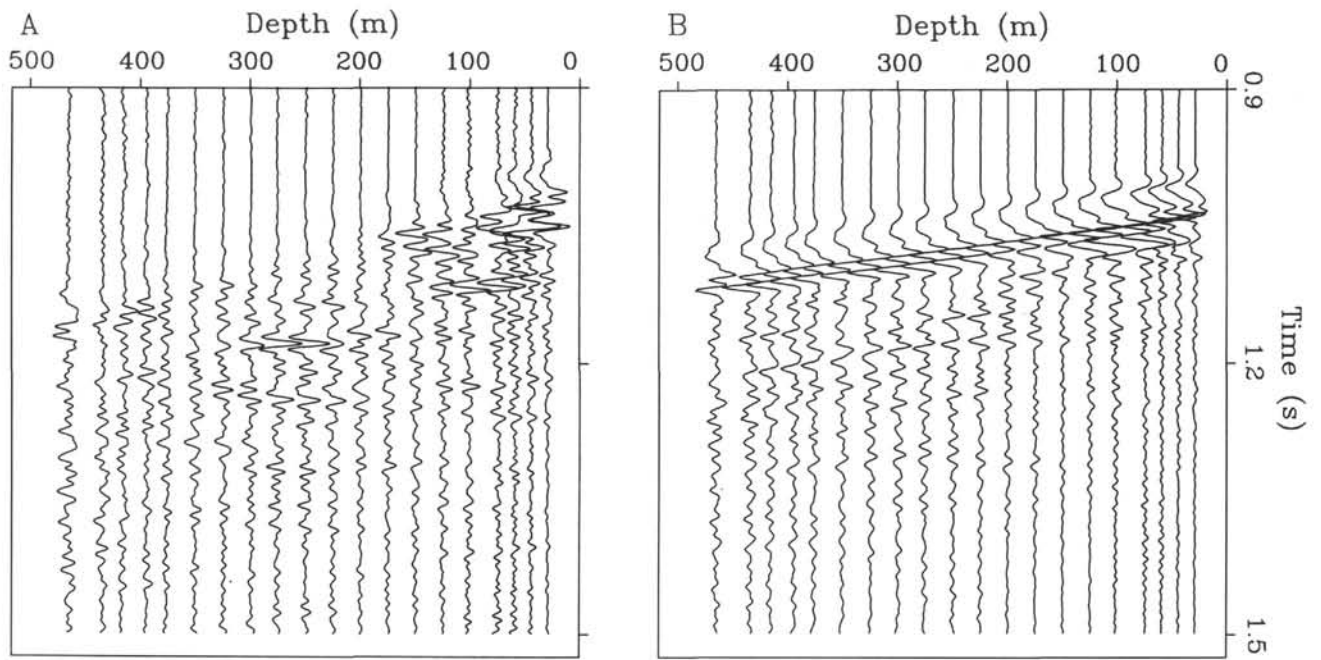


Figure 3. Water-gun record section processed by stacking and F-K filtering. A. Up-going wavefield. Timing adjusted as in Figure 2A. B. Down-going wavefield.

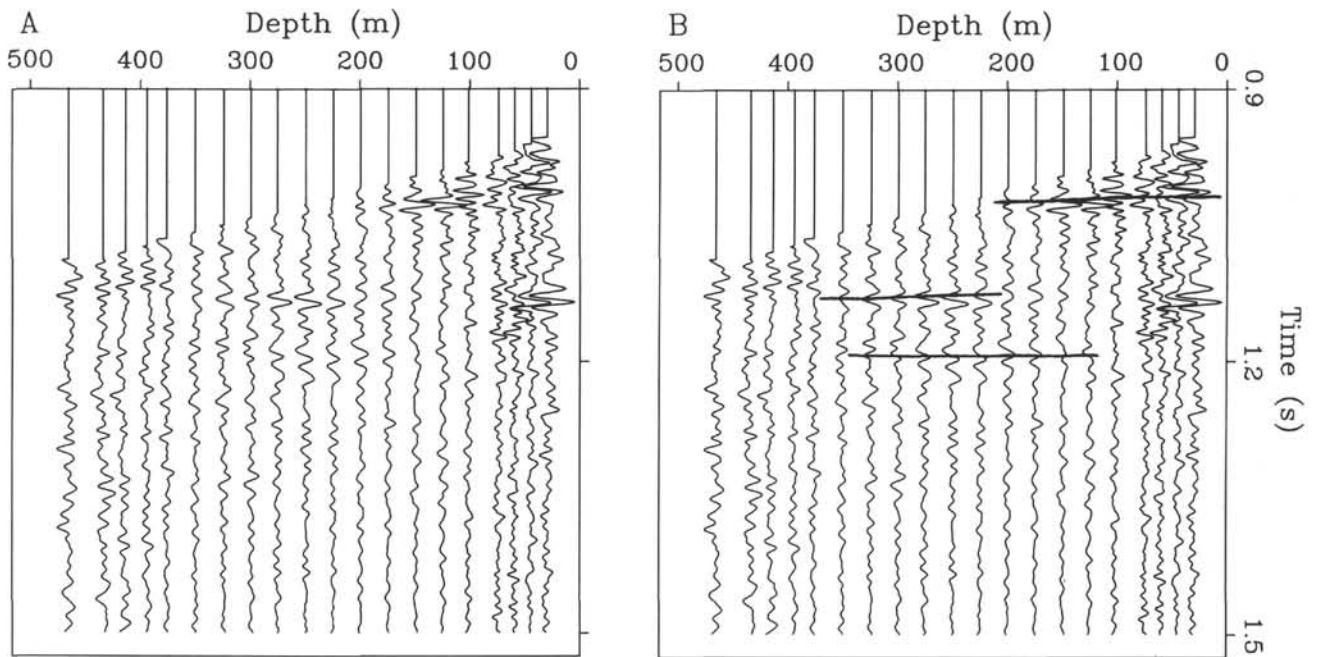


Figure 4. Deconvolved air-gun record section. Timing adjusted as in Figure 2A. A., B. Same sections, except that A has addition of authors' interpretation of reflection events.

0.16 s includes the primary pulse. For the air gun, we chose a length of 0.45 s to include three cycles of the bubble pulse.

Figures 4 and 5 show the deconvolved sections. Two improvements in data quality are immediately obvious. The water-gun first arrival is impulsive, rather than a low-amplitude precursor. In addition, the air-gun bubble pulse (period of ~0.17 s in Fig. 2B) has been removed.

INTERVAL VELOCITIES

Interval velocities computed using the VSP traveltimes in Shipboard Scientific Party (1989) were smoothed by a five-point moving average (~115 m or ~55 Hz at 6.5 km/s). Figure 6 depicts these data plotted vs. depth with the lithologic column from Hole 735B. Low velocities are associated with

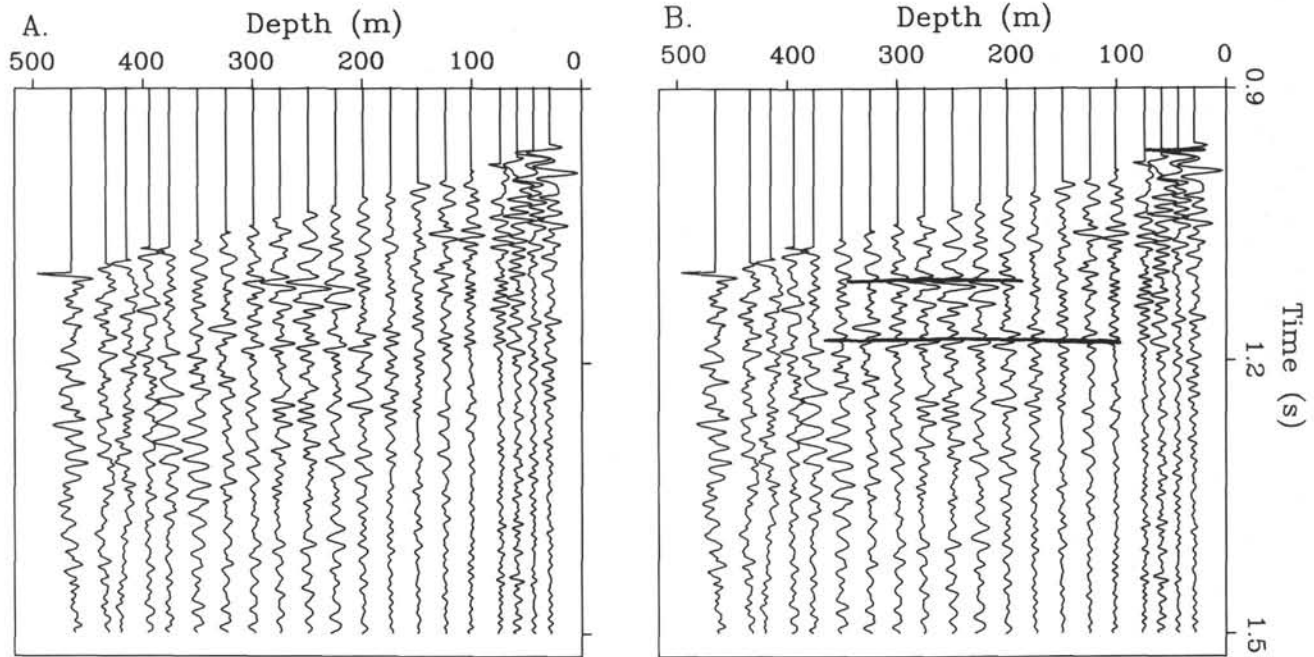


Figure 5. Deconvolved water gun record section. Timing adjusted as in Figure 2A. A., B. Same sections, except that A has addition of authors' interpretation of reflection events.

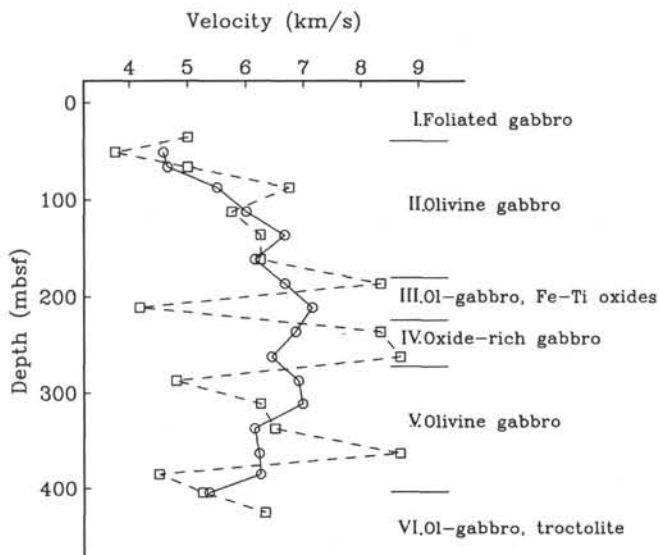


Figure 6. Interval velocities from one-way traveltimes to VSP receiver depths (Shipboard Scientific Party, 1989). Dashed line connecting squares represents raw velocities. These velocities are sensitive to small subjective errors in selection of seismic arrivals. Solid line connecting circles indicates velocities after smoothing by a five-point moving average and is a more reliable indication of seismic velocity. Numbered annotations are lithologic units from Shipboard Scientific Party (1989).

lithologic Units I and VI. These units contain most of the brittle and plastic deformation structures observed in the borehole (Shipboard Scientific Party, 1989). Nearly one-half of the cracks and joints observed occur in Unit I. The dip in smoothed velocity near the base of Unit II correlates with a brecciated zone that has been interpreted as a fault surface at

the contact between Units II and III. We suggest that low seismic velocities are weakly associated with deformation zones in the borehole. Kirby et al. (unpublished data) compare these smoothed velocities to velocities obtained by laboratory measurements and sonic logging.

SEISMIC STRATIGRAPHY

The time-shifted seismograms in Figures 2A, 3A, 4, and 5 may be viewed as seismic reflection profiles in two-way traveltimes at a single location. The depth to reflection events may be found by following the event toward deeper receiver depths to where the event intercepts the first arrival. The depth of the receiver at that intercept is the depth of the reflector. Below the bottom of the hole, the depth below a particular receiver to a reflector may be found by extrapolating the average velocity for the borehole (6.5 km/s) downward and by measuring time since the first arrival of the down-going wave at that receiver.

The amplitudes of some reflections discussed below are not coherent for all receiver depths. Difficulties in tracing events across the sections may be due in part to phase shifting caused by clipping of the air-gun data, to interference from ship and pipe-banging noises when the receiver was clamped within the top 60 to 80 m of the borehole, or to waveform distortion introduced during F-K filtering. The apparent lack of coherence between seismograms may also result from real differences in power received at different borehole depths. The reflective surfaces may be laterally variable in dimensions and/or in reflective character. As the depth of the receiver changes, the distance to the reflection surface changes. As a result, the Fresnel Zone, the area from which reflected waves will constructively interfere, will also change. We computed the radius, r , of the first Fresnel Zone using Hardage's equation (1983),

$$r^2 = \frac{\lambda ab}{a + b} \quad (1)$$

where λ = wavelength,

a = distance from source to reflecting surface, and

b = distance from receiver to reflecting surface.

We assumed a uniform velocity of 6.5 km/s and included the water layer in the source-reflecting surface separation. The radius of the Fresnel Zone for a reflector at 225 mbsf (see below) at 10 Hz can range from 328 m for a receiver at 20 mbsf to 113 m at 200 mbsf. At 20 Hz, the radius ranges from 232 to 80 m. Studies of layered gabbros in ophiolites have shown lateral variations in lithology and structure on these scales (e.g., Casey et al., 1981). In deeper sequences that include ultramafic rocks, the lateral variations are clearly sufficient to change the amplitudes and depths of reflections (Collins et al., 1986). We attribute some of the trace-to-trace variations in reflector amplitude and waveform in our sections to the laterally irregular nature of the reflecting surfaces. Synthetic seismogram modeling to demonstrate this contention, such as that of Collins et al., is beyond the scope of this study.

The seismic image obtained using the air gun differs from that generated using the water gun, primarily in the coherency between receivers of the reflection at ~ 1.02 s traveltime. We attribute these differences to dissimilar spectral contents of the down-going energy produced by each type of gun (Fig. 1) and to interlayering of impedance contrasts on depth scales less than the seismic wavelength. The down-going energy from the air gun peaks at ~ 8 Hz (Fig. 1) with a wavelength of ~ 810 m. The energy of the water gun travels at higher frequencies (20–35 Hz) and shorter wavelengths (185–325 m). We suspect that the absence of a coherent reflection at 1.02 s in the water-gun data (see below) is the result of destructive interference between the primary reflection and a pegleg multiple from within Unit IV. The pegleg multiple was not generated by the considerably longer air-gun signal. Testing this hypothesis by generating synthetic VSP seismograms is beyond the scope of this study.

In both the F-K filtered sections and the deconvolved sections, considerably more energy returns from the upper half of the hole than from the lower half (Figs. 2A, 3A, 4, and 5). Two reflectors can be traced: one at 50 to 70 mbsf in the water-gun data and one at 225 to 250 mbsf in the air-gun data. Smaller velocity changes deeper in the hole do not appear to have produced coherent reflections. The shallow reflection appears to correlate with the base of the foliated gabbros (Unit I/Unit II boundary). Across this boundary, the frequency of observations of plastic deformation decrease downward (Fig. 7 in Shipboard Scientific Party, 1989), laboratory-measured velocity increases (Fig. 64 in Shipboard Scientific Party, 1989), and both the density and velocity measured by logging increase (Figs. 74 and 85 in Shipboard Scientific Party, 1989). The top of the deeper reflection correlates with a downward increase in deformation and an increase in density at the top of the Fe-Ti rich gabbro (Unit IV). Velocity and density also change significantly in the logs at the base of this unit at 260 to 270 mbsf. The long wavelengths and receiver spacing used in this study are probably insufficient to resolve separate reflections from the top and bottom of Unit IV. Layer resolution is a complex function of source spectrum, impedance, and layer thickness (Kallweit and Wood, 1982; de Voogd and den Rooijen, 1983). Experiments at resolving thin beds, however, suggest that with good signal-to-noise conditions beds of greater than about one-quarter wavelength can be resolved seismically (Widess, 1973; Waters, 1978). In the case of the air-gun data, this limit is a bed having a thickness of ~ 200 m. It is probable that the reflected energy at 225 to 250 mbsf is a complex response to both the top and bottom of the Fe-Ti rich zone or to a structural surface coincident with the bed.

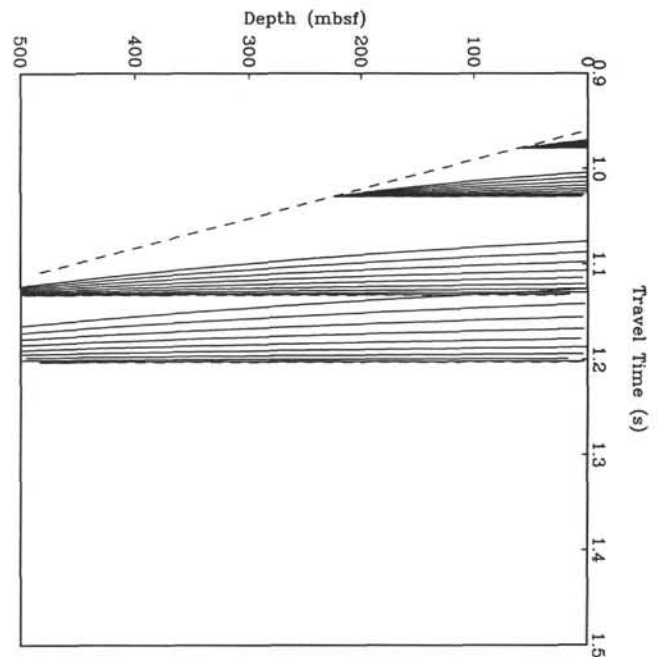


Figure 7. Synthetic traveltimes for dipping reflectors obtained by ray tracing from a sea-surface source to dipping reflector surfaces at four borehole depths. Scale is similar to that in Figures 2 through 5. Upper dashed line indicates direct, down-going arrival at borehole receivers. Lower dashed line in each of four groups of curves represents reflection from horizontal surface. Solid lines are reflections from surfaces with dips ranging from 5° to 45° in 5° increments. Four groups of traveltime curves shown were computed for reflectors that intersect the borehole at 60, 225, 560, and 790 mbsf.

Below the bottom of the hole, a high-amplitude event occurs at ~ 1.11 s two-way traveltime, and a fainter reflector occurs at 1.17 to 1.19 s on both air- and water-gun record sections. Using a velocity of 6.5 km/s and a two-way traveltime to the base of the hole of 1.09 s, the depths of the impedance changes producing the two reflections are 565 mbsf and 760 to 825 mbsf, respectively. Neither reflection is apparent at receiver depths greater than 350 mbsf in the deconvolved section (Figs. 4 and 5), but both can be traced to the deepest receiver in the F-K filtered air-gun section (Fig. 2A). Owing to poor signal-to-noise ratios caused by tool slippage in the lower 100 m of the borehole, the deconvolution operator may have removed this reflection. The amplitude of both reflections diminishes above 200-mbsf receiver depth. The absence of significant energy from receivers above 200 m may be due to downward reflection by the strong velocity and density change at the base of Unit IV, to limited size of the reflection surface, or to lateral variations in the velocity and density contrasts across the surface at scales of tens to hundreds of meters.

In Figures 4B and 5B, traveltimes to the four reflectors appear to be independent of receiver depth and, thus, indicative of flat reflector surfaces (Hardage, 1983, p. 225). To test this inference and the sensitivity of arrival times to reflector dip, we computed synthetic traveltimes for dipping reflectors and compared these arrivals to the processed data. Our model included a homogeneous water layer having a velocity of 1.5 km/s, a flat seafloor, and a homogeneous basement with a velocity of 6.5 km/s over a uniformly dipping surface. We assumed a vertical borehole and a zero-offset source. Figure 7 shows synthetic traveltimes for reflectors that intersect the hole at depths of 60, 225, 560, and 790 m and that dip 0° to 45°

from the horizontal. We matched model curves to the reflectors marked in Figures 4B and 5B. The number of receiver stations that recorded arrivals from the shallowest reflector are insufficient to estimate a dip. The dip of the 225-m reflector is uncertain as well, because amplitude changes and possible phase reversals with receiver depth make selection of the reflector uncertain. The 560- and 790-m reflectors have dips of 20° to 25° and 10° to 15°, respectively. For all reflectors, a large uncertainty in dip exists. Dips up to 30° to 40° might be accommodated at any of the four events by small changes in the way the trace follows amplitude peaks. Figure 7 also shows that a dipping reflector appears more shallow than the reflection from a horizontal surface that intercepts the hole at the same depth by a traveltime proportional to the dip and the depth to the surface at the borehole. Using the measured dips for the 560- and 790-m reflectors, we computed depth corrections of ~80 and ~50 m, respectively, placing the actual horizons at ~640 and 810 to 850 mbsf.

DISCUSSION

The origin of the VSP seismic sequence at Site 735 is not clear. All four events could be reflections from within "normal" ocean crust. The deeper events might instead be reflections from a shallow transition to upper mantle or from structures formed during tectonic uplift of the ridge, such as faults or serpentinite bodies. We lack an image of the internal structure of the ridge from multichannel seismic profiling and refraction velocities with which we could more easily place the VSP reflection sequence and, thus, the borehole stratigraphy in a regional geologic framework.

We tentatively attribute the VSP sequence to a shallow transition to mantle. In lieu of seismic data, our interpretation is influenced by geophysical surveys of the Atlantis II Fracture Zone, lithostratigraphy of Site 735, and comparison to Moho reflections from the western North Atlantic. Based on modeling of gravity data, lithology of dredge samples, structural interpretation of topography, and lithostratigraphy of Site 735, Dick, Schouten, et al. (this volume) argue that the crust at Site 735 is thin, composed of lower crustal rocks formed at a near-"normal" spreading center and is underlain by shallow upper mantle. The two deepest events in the VSP data may be reflections from a relatively abrupt igneous transition or from a low-angle fault contact between crust and mantle. The closeness of the deepest reflectors (~230 m) indicates a transition having a thickness on the low end of the range reported from ophiolite studies and from wide-angle reflection-refraction experiments (e.g., Spudich and Orcutt, 1980; Casey et al., 1981; Collins et al., 1986). Our data can accommodate dips of 30° to 40° and, thus, is consistent with either the low-angle fault zone proposed by Dick, Schouten, et al. (this volume) or Moho topography of several hundred meters apparent in ophiolites (Collins et al., 1986) and in North Atlantic multichannel profiles (NAT Group, 1985; McCarthy et al., 1988).

Published modeling studies indicate that both lithologic and structural contacts may produce reflections of observable amplitude. Collins et al. (1986) demonstrated that lithologic transitions between lower ocean crust and upper mantle can produce reflections similar in character to "Moho" reflections in oceanic multichannel profiles. On the other hand, modeling studies of major continental thrust faults suggest that faults are more likely to cause reflections with high enough amplitudes to be observed than are lithologic boundaries (Jones and Nur, 1984; Christensen and Szymanski, 1988). Deformation zones associated with faulting produce high-amplitude reflections resulting from occurrence of mylonite, interlayering of undeformed rock, and

rock having high concentrations of phyllosilicates oriented parallel to foliation, and to thin zones of high fluid pore pressures (Jones and Nur, 1984; Matthews and Cheadle, 1986; Christensen and Szymanski, 1988). Thus, the nature of the transition at Site 735 is uncertain. Compared to the western North Atlantic sequences of McCarthy et al. (1988), the total traveltime thickness of the VSP sequence (~0.22 s) is similar to that of faults that penetrate layers 2 and 3, but is on the low end of the range in thickness of lower crustal and Moho sequences. Thus, it seems unlikely that the upper 800 m at Site 735 includes both a major crustal fault of the type seen in the western North Atlantic seismic images and a typical Moho transition.

Our interpretation of a shallow mantle reflection and the structural model proposed by Dick, Schouten, et al. (this volume) for the transverse ridge at the Atlantis II Fracture Zone (ridge offset of 210 km) is similar to that found at large offset fracture zones in the Atlantic, but differs from smaller offset fracture zones. Based on explosive refraction data, Detrick and Purdy (1980) and Cormier et al. (1984) suggested that high-velocity material occurred within the transverse ridge north of the Kane Fracture Zone (offset of 150 km), but they could not resolve the thickness of overlying crust. Using gravity and bathymetry data, Loudon and Forsyth (1982) determined that the crust beneath the ridge was about one-half normal crustal thickness (~3 km). Beneath the north transverse ridge (Hecate Bank) at the southern Charlie Gibbs Fracture Zone (offset of 125 km), Whitmarsh and Calvert inferred material with high density and low velocity characteristic of upper mantle rock at 1.3 to 1.5 km below seafloor. At the Oceanographer Fracture Zone (offset of 120 km), refraction data indicate thinning of crust toward the fracture zone and anomalous crust below the fracture zone trough, but do not indicate unusually thin crust below the transverse ridge (Sinha and Loudon, 1983, Line B). At fracture zone 1 (offset of 25 km) south of the Oceanographer, White et al. (1984) found thin crust and low velocities only beneath the trough; normal crustal velocities occur beneath the bathymetric high to the north. Finally, at the Blake Spur Fracture Zone (offset of 8 km), McCarthy et al. (1988) showed that the depth to a seismic event, interpreted as Moho, increases beneath the fracture zone. In summary, crust beneath transverse ridges is thinner (<1–2 km) at fracture zones with offsets greater than 125 km, whereas transverse ridges at fracture zones with offsets of less than 120 km have structures that are transitional between normal crust and that beneath the fracture zone trough.

CONCLUSIONS

We imaged two reflections from within the borehole sequence (at 50–70 and 225–250 mbsf) and two reflections from below (at 560 and 760–825 mbsf). Different amplitude and phase of the reflections at different receiver depths are related, at least in part, to limited dimensions of the reflecting surfaces and to lateral changes in the physical property contrasts across the surfaces. The two shallow reflections correlate with changes in lithology and deformation features at unit boundaries. The origin of the deeper reflectors is uncertain until further drilling or geophysical data can be collected to place the sequences in a geologic framework. We tentatively correlate the VSP reflection sequence to a transition from lower crust to upper mantle, but are uncertain whether this transition is a faulted or igneous contact. Combined with geophysical studies at North Atlantic fracture zones, our interpretation suggests that transverse ridges having offsets greater than ~120 to 125 km are anomalous in having exceptionally thin crust (<1–2 km).

ACKNOWLEDGMENTS

Collection and processing of the VSP data were supported by Ocean Drilling Program/Texas A&M University, Purchase Order Nos. 20094, 20108, and 20209. We thank the officers, drilling crew, and laboratory technicians of the *JOIDES Resolution* for their generous assistance at sea. Ted Gustafson rigged and operated the guns during the VSP, and Jenny Glasser operated the acquisition system. Discussions with Chris Bradley greatly assisted data processing. C. Bradley, S. Holbrook, and an anonymous reviewer provided helpful comments about the manuscript.

REFERENCES

- Casey, J. F., Dewey, J. F., Fox, P. J., Karson, J. A., and Rosenkrantz, E., 1981. Heterogeneous nature of oceanic crust and oceanic mantle: perspective from the Bay of Islands Ophiolite Complex. In Emiliani, C. (Ed.), *The Sea*, Vol. 7: New York (Wiley), 305–338.
- Christensen, N. I., and Szymanski, D. L., 1988. Origin of reflections from the Brevard Fault Zone. *J. Geophys. Res.*, 93:1087–1102.
- Christie, P. A. F., Hughes, V. J., and Kennett, B. L. N., 1983. Velocity filtering of seismic reflection data. *First Break*, 1:9–24.
- Collins, J. A., Brocher, T. M., and Karson, J. A., 1986. Two-dimensional seismic reflection modeling of the inferred fossil ocean crust/mantle transition in the Bay of Islands ophiolite. *J. Geophys. Res.*, 91:12520–12538.
- Cormier, M. H., Detrick, R. S., and Purdy, G. M., 1984. Anomalous thin crust in oceanic fracture zones: new seismic constraints from the Kane Fracture Zone. *J. Geophys. Res.*, 89:10249–10266.
- Detrick, R. S., and Purdy, G. M., 1980. The crustal structure of the Kane Fracture Zone from seismic refraction studies. *J. Geophys. Res.*, 85:3759–3777.
- de Voogd, N., and den Rooijen, H., 1983. Thin-layer response and spectral bandwidth. *Geophysics*, 48:12–18.
- Dey-Sarker, S. K., and Wiggins, R. A., 1976. Source deconvolution of teleseismic Pwave arrivals between 14° and 40°. *J. Geophys. Res.*, 81:3633–3641.
- Hardage, B. A., 1983. *Vertical Seismic Profiling, Part A: Principles*: London (Geophysical Press).
- Jones, T., and Nur, A., 1984. The nature of seismic reflections from deep crustal fault zones. *J. Geophys. Res.*, 89:3153–3171.
- Kallweit, R. S., and Wood, L. C., 1982. The limits of resolution of zero-phase wavelets. *Geophysics*, 47:1035–1046.
- Karson, J. A., and Elthon, D., 1987. Evidence for variations in magma production along oceanic spreading centers: a critical appraisal. *Geology*, 15:127–131.
- Karson, J. A., and Fox, P. J., 1986. Geological and geophysical investigation of the Mid-Cayman Spreading Centre: seismic velocity measurements and implications for the constitution of layer 3. *Geophys. J. R. Astron. Soc.*, 85:389–411.
- Langston, C. A., 1979. Structure under Mount Ranier, Washington, inferred from teleseismic body waves. *J. Geophys. Res.*, 84:4749–4762.
- Lee, M. W., and Balch, A. H., 1983. Computer processing of vertical seismic profile data. *Geophysics*, 48:272–287.
- Louden, K. E., and Forsyth, D. W., 1982. Crustal structure and isostatic compensation near the Kane Fracture Zone from topography and gravity measurements—1. Spectral analysis approach. *Geophys. J. R. Astron. Soc.*, 68:725–750.
- McCarthy, J., Mutter, J. C., Morton, J. L., Sleep, N. H., and Thompson, G. A., 1988. Relic magma chamber structures preserved within the Mesozoic North Atlantic. *Geol. Soc. Am. Bull.*, 100:1423–1436.
- Matthews, D. H., and Cheadle, M. J., 1986. Deep reflections from the Caledonides and Variscides west of Britain and comparison with the Himalayas. In Barazangi, M., and Brown, L. (Eds.), *Reflection Seismology: A Global Perspective*: Washington (Am. Geophys. Union), Geodyn. Ser., 14:281–292.
- Minshull, T. A., White, R. S., Buhl, P., Mutter, J., Detrick, R. S., and Morris, E., 1988. Investigation of variations in oceanic crustal structure across a small offset fracture zone: Blake Spur Fracture Zone Experiment. *Eos*, 69:1441.
- Mutter, J. C., Detrick, R. S., and North Atlantic Study Group, 1984. Multichannel evidence for anomalously thin crust at Blake Spur fracture zone. *Geology*, 12:534–537.
- North Atlantic Study Group, 1985. North Atlantic Transect: a wide-aperture, two-ship multichannel seismic investigation of the oceanic crust. *J. Geophys. Res.*, 90:10321–10341.
- Ross, W. S., and Shah, P. M., 1987. Vertical seismic profile reflectivity: ups over downs. *Geophysics*, 52:1149–1154.
- Shipboard Scientific Party, 1989. Site 735. In Robinson, P. T., Von Herzen, R., et al., *Proc. ODP, Init. Repts.*, 118: College Station, TX (Ocean Drilling Program), 89–816.
- Sinha, M. C., and Loudon, K. E., 1983. The Oceanographer Fracture Zone—1. Crustal structure from seismic refraction studies. *Geophys. J. R. Astron. Soc.*, 75:713–736.
- Spudich, P., and Orcutt, J., 1980. A new look at the seismic velocity structure of the oceanic crust. *Rev. Geophys. Space Phys.*, 18:627–645.
- Waters, K. H., 1978. *Reflection Seismology*: New York (Wiley).
- White, R. S., Detrick, R. S., Sinha, M. C., and Cormier, M. H., 1984. Anomalous seismic crustal structure of oceanic fracture zones. *Geophys. J. R. Astron. Soc.*, 85:779–798.
- White, R. S., Detrick, R. S., Mutter, J., Buhl, P., Minshull, T. A., and Morris, E., 1988. Lower crustal layering, dipping reflectors, and fracture zone structure in Mesozoic oceanic crust. *Eos*, 69:1440.
- Whitmarsh, R. B., and Calvert, A. J., 1986. Crustal structure of Atlantic fracture zones—1. The Charlie-Gibbs Fracture Zone. *Geophys. J. R. Astron. Soc.*, 85:107–138.
- Widess, M. B., 1973. How thin is a thin bed? *Geophysics*, 38:1176–1180.

Date of initial receipt: 30 June 1989

Date of acceptance: 4 June 1990

Ms 118B-141